



FIA 2018

XI Congreso Iberoamericano de Acústica; X Congreso Ibérico de Acústica; 49º Congreso Español de Acústica -TECNIACUSTICA'18-
24 al 26 de octubre

TIRE-PAVEMENT INTERACION NOISE: EXPERIMENTS AND MODEL DEVELOPMENT

PACS: 43.50.Lj TRANSPORTATION NOISE SOURCES: AIR, ROAD, RAIL, AND MARINE VEHICLES

McBride, Sterling; Spies, Lucas; Burdisso, Ricardo
Institución: Department of Mechanical Engineering, Virginia Tech
Dirección: 635 Prices Fork Road, 445 Goodwin Hall
Población: Blacksburg, Virginia 24060
País: Estados Unidos de América
Tel: +1 609 532 0427
E-Mail: sterling.mcbride@vt.edu; lucass19@vt.edu; rburdiss@vt.edu

Keywords: Tire-Pavement Interaction Noise,

ABSTRACT.

IN THIS WORK, AN OVERVIEW OF THE RESEARCH WORK ON TIRE PAVEMENT INTERACTION NOISE (TPIN) PERFORMED AT THE DEPARTMENT OF MECHANICAL ENGINEERING AT VIRGINIA TECH IS PRESENTED. AS PART OF THE RESEARCH EFFORT A LARGE EXPERIMENTAL CAMPAIGN WAS UNDERTAKEN. NOISE AND PAVEMENT PROFILE DATA WAS COLLECTED FOR 42 TIRES AND 27 DIFFERENT TYPES OF PAVEMENTS. IT WAS POSSIBLE TO SEPARATE TPIN INTO TREAD-PATTERN AND NON-TREAD PATTERN RELATED NOISE. TWO DIFFERENT NOISE PREDICTION MODELS ARE UNDER DEVELOPMENT. THE FIRST ONE IS A SEMI-EMPIRICAL APPROACH AND THE SECOND ONE IS ANALYTICAL.

RESUMEN.

EN ESTE TRABAJO SE PRESENTA UN RESUMEN DE LA INVESTIGACIÓN REALIZADA POR EL DEPARTAMENTO DE INGENIERÍA MECÁNICA DE VIRGINIA TECH SOBRE RUIDO PRODUCIDO POR LA INTERACCIÓN NEUMÁTICO-PAVIMENTO. UNA GRAN CANTIDAD DE DATOS EXPERIMENTALES FUERON ADQUIRIDOS, INCLUYENDO RUIDO DE 42 NEUMÁTICOS DISTINTOS Y 27 PERFILES DE PAVIMENTOS. FUE POSIBLE SEPARAR EL RUIDO EN DOS COMPONENTES PRINCIPALES. UNA DE ELLAS DEPENDIENTE Y LA OTRA INDEPENDIENTE DE LA GEOMETRÍA DEL DIBUJO DE LA CUBIERTA. ACTUALMENTE DOS MODELOS PARA PREDECIR LOS NIVELES DE RUIDO DEBIDO A ESTE FENÓMENO SE ENCUENTRAN EN DESARROLLO, UNO DE ELLOS SEMI-EMPÍRICO, Y EL OTRO ANALÍTICO.

1. INTRODUCTION

Highway traffic is considered one of the most important urban noise sources, especially in the vicinity of highly populated areas. It can be divided in different sub-sources like engine/drive train noise, exhaust noise, aerodynamic noise, and tire pavement interaction noise (TPIN). However, the latter is dominant at speeds above 30 mph¹. For this reason research on tire noise has become very important, especially among the tire manufacturing community. An overview of the investigation effort on TPIN taken place at Virginia Tech is presented in this work. The large amount of experimental data collected has uncovered specific characteristics of TPIN regarding tread-pattern and non-tread pattern noise components. Relationships between non-tread pattern noise and measured pavement profiles have been identified. Finally, important correlation

FIA 2018

XI Congreso Iberoamericano de Acústica; X Congreso Ibérico de Acústica; 49º Congreso Español de Acústica -TECNIACUSTICA'18-
24 al 26 de octubre

parameters between tire construction (i.e. hardness and geometry) and rotational velocity with the produced noise have also been defined.

Mathematical computation tools can be used to produce fairly accurate TPIN predictions^{2,3}. Specifically, Artificial Neural Networks (ANNs) are able capture typical TPIN behavior including its complex nature and nonlinearities. On the other hand, analytical methods model the complete tire structure using shells or plates, to later compute the produced noise. Models such as these are desirable for providing further physical insight. Both approaches have been explored at Virginia Tech and will be briefly described in this work.

2. EXPERIMENTS

A large experimental campaign was carried out by the Mechanical Engineering department at Virginia Tech. TPIN noise was measured at two different sites: (1) US 460 east and west bound and (2) Virginia Tech Transportation Institute (VTTI) Smart Road. Both are located in Blacksburg, VA, USA (see Figure 1a and 1b). The US 460 test section consists of a 1.3 mile straight section with dense graded hot mix asphalt. On the other hand, the smart road is a 2.2 mile controlled-access test track that consists of 26 types of pavements including 15 mixed asphalt sections, 8 concrete sections, 3 bridges and 7 concrete grooved sections.

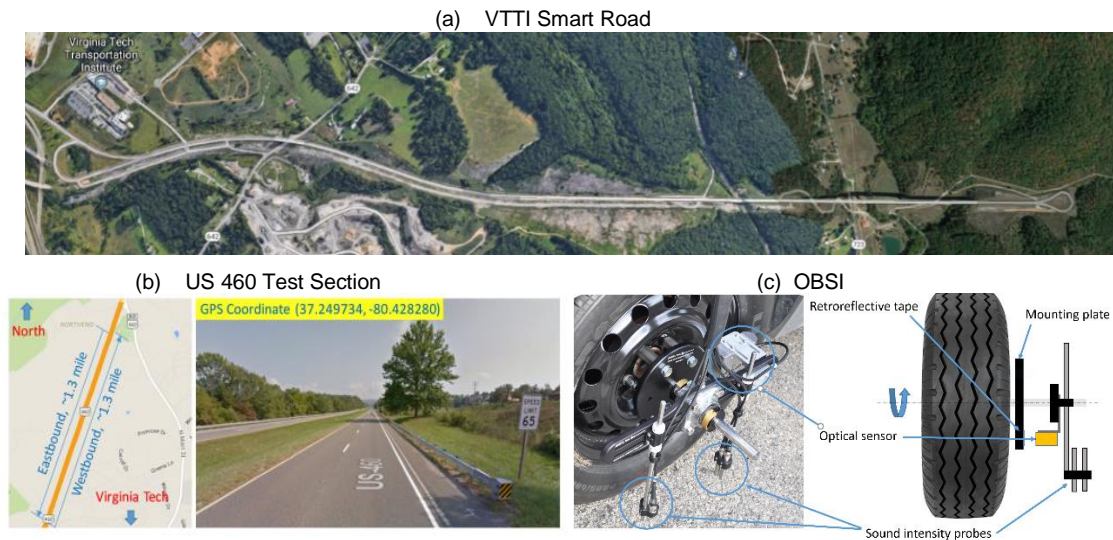


Figure 1 – (a) VTTI Smart Road, (b) US 460 Test Section, (c) OBSI.

The Onboard Sound Intensity (OBSI) system shown in Figure 1c was used for all noise measurements. It consists of 2 sound intensity probes located at the leading and trailing edges of the rolling tire. In addition, an optical sensor was mounted that enabled the system to capture a one-per-revolution signal. The entire system follows the standard AASHTO TP-76⁴. The OBSI system was mounted on two different vehicles, a 2017 Chevrolet Tahoe for large tires ($\phi > 800$ mm) and a 2012 Chevrolet Impala for smaller tires ($\phi < 700$ mm). Both are shown in Figure 2a.



Figure 2 – (a) Test Vehicles, (b) SCRIM Truck.

FIA 2018

XI Congreso Iberoamericano de Acústica; X Congreso Ibérico de Acústica; 49º Congreso Español de Acústica -TECNIACUSTICA'18-
24 al 26 de octubre

A total of 42 tires of various sizes and manufacturers were tested for 5 vehicle speeds between 45 to 65 mph. An acceleration test between these two velocities was also performed. A hardness test for all tires showed a wide range between 56 to 79 Shore A. In addition 3 different pressures were used for testing (26, 32 and 40 psi). Finally, the ambient temperature ranges for all tests was within 37°F to 86°F. Pavement profile data was also collected on both sites using a Sideway-Force Coefficient Routine Investigation Machine (SCRIM) shown in Figure 2b. This equipment was used to scan all pavement surfaces with a high resolution of 0.5 to 1 mm.

3. EXPERIMENTAL RESULTS

The collected TPIN data uncovered many characteristics of its behavior. One of the most significant showed the existence of two separate components of noise. The tire construction defines tread impact and air pumping behavior, both periodic with the speed of rotation of the tire. This is evident in Figure 3a, where a noise spectrogram during an acceleration test on US 460 reveals the first component of noise that depends on the vehicle's speed. Thus, it can be inferred that this varying component is related to the tread pattern. A second component of noise is also observed and is clearly not related to the periodic tread pattern. This component is due to the pavement. This is referred as non-tread pattern noise².

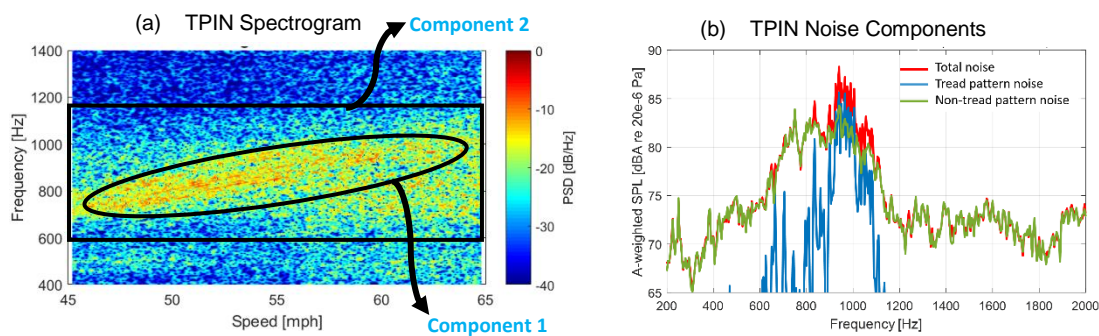


Figure 3 – (a) TPIN spectrogram measured in acceleration test at US 460, (b) Separated noise components for a Michelin X-ICE 13 of size 215/60R16 - US 460.

The OBSI's optical sensor signal is used to separate both noise components. It provides a one-per revolution signal that defines the noise related to the rotation of the tire. Therefore, by coherently averaging the spectral TPIN content for multiple completed revolutions of the tire, component 1 is defined. This is then subtracted from the total to obtain component 2. An example of the separated noise components and the total is shown in Figure 3b. It can be observed that tread-pattern noise is dominant ~1000 Hz, while non-tread pattern noise is broad band dominant at lower and higher frequencies. This behavior is observed for most tires tested, especially for those with more aggressive tread designs such as winter tires.

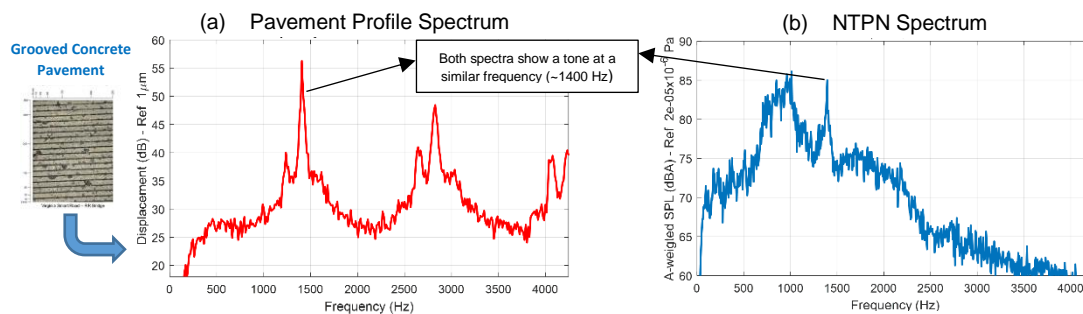


Figure 4 – (a) Pavement Profile Spectrum for a grooved concrete pavement from VTTI Smart Road, (b) Corresponding section non-tread pattern noise for a Michelin X-ICE 13 of size 215/60R16.

The SCRIM truck was used to measure the pavement profile for all test sections. The spectral content for all of them was computed and compared with the corresponding noise data. The

FIA 2018

XI Congreso Iberoamericano de Acústica; X Congreso Ibérico de Acústica; 49º Congreso Español de Acústica -TECNIACUSTICA'18-
24 al 26 de octubre

results show that for transverse grooved pavements the first tone appears at a similar frequency as in the non-tread pattern noise spectrum (see Figure 4). Thus, noise measurements that include the component separation has the potential of capturing pavement distress and characterizing groove geometry on pavement surfaces.

Finally, two important conclusions are observed from the separation of the noise into the two components. The tread pattern noise is a function of only the tread pattern while the non-tread pattern noise is a function of only the pavement.

4. TPIN MODELS

ANN Semi-Empirical Prediction Model

The experimental data was used to develop an ANN based semi-empirical noise model. Two ANNs have been developed to predict TPIN for both tread pattern noise (ANN_{TPN}) and non-tread pattern noise (ANN_{NTPN}) independently. Table 1 shows the inputs and outputs for each one.

Table 1 – Inputs and outputs for each ANN_{TPN} and ANN_{NTPN}

Layer	ANN _{TPN}	ANN _{NTPN}
Input	<ul style="list-style-type: none"> Tread pattern profile spectrum. Air volume velocity spectrum. Rotational speed. 	<ul style="list-style-type: none"> Rubber hardness (Shore A). Rotational speed. Pavement profile.
Output	<ul style="list-style-type: none"> Acoustic sound pressure (p_{rms}^2) order spectrum 	<ul style="list-style-type: none"> Acoustic sound pressure (p_{rms}^2) frequency spectrum.

To predict the tread pattern noise, the 3D tread profile is needed typically obtained using a 3D laser scanner, as shown in Figure 5a. Two tread pattern noise generation mechanisms are then identified: (1) tread impact due to the tread profile irregularities, shown in the example in Figure 5b and (2) air pumping due to the air volume changes within the tread grooves of the contact area, seen in Figure 5d. In order to characterize the tread impact mechanism, the tread profile for each circumference section was Fourier transformed and then coherently averaged (accounting for phase) across the tire width, resulting in the coherent tread profile spectrum shown in Figure 5c. For the air pumping mechanism, the air volume velocity i.e. the time derivative of the air volume is Fourier transformed, resulting in the air volume velocity spectrum (see Figure 5e).

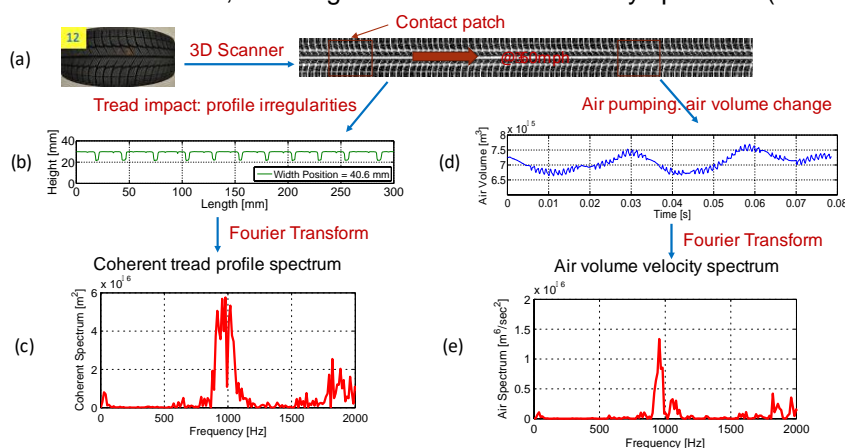


Figure 5 – Illustration of tread pattern analysis.

Since tread pattern noise is periodic in relation to tire rotation, order power spectrum is preferred instead of frequency power spectrum. This approach makes the power spectrum independent of the speed.

Both ANNs were configured to provide all positive p_{rms}^2 outputs. The use of a standard pure linear transfer function could result in negative output values. For this reason a hybrid transfer function combining both symmetric sigmoid and pure linear functions was implemented in the ANN output

FIA 2018

XI Congreso Iberoamericano de Acústica; X Congreso Ibérico de Acústica; 49º Congreso Español de Acústica -TECNIACUSTICA'18-
24 al 26 de octubre

layer. Results of the constructed TPIN prediction tool were validated against measurements from 8 tires that were exclusively used for validation (not used for training of ANNs). The predicted total, tread-pattern, and non-tread pattern noise spectrums showed good agreement with measurements. Figure 6 shows these spectrums for a 215/60R16 Bridgestone Winterforce tire at 5 different speeds.

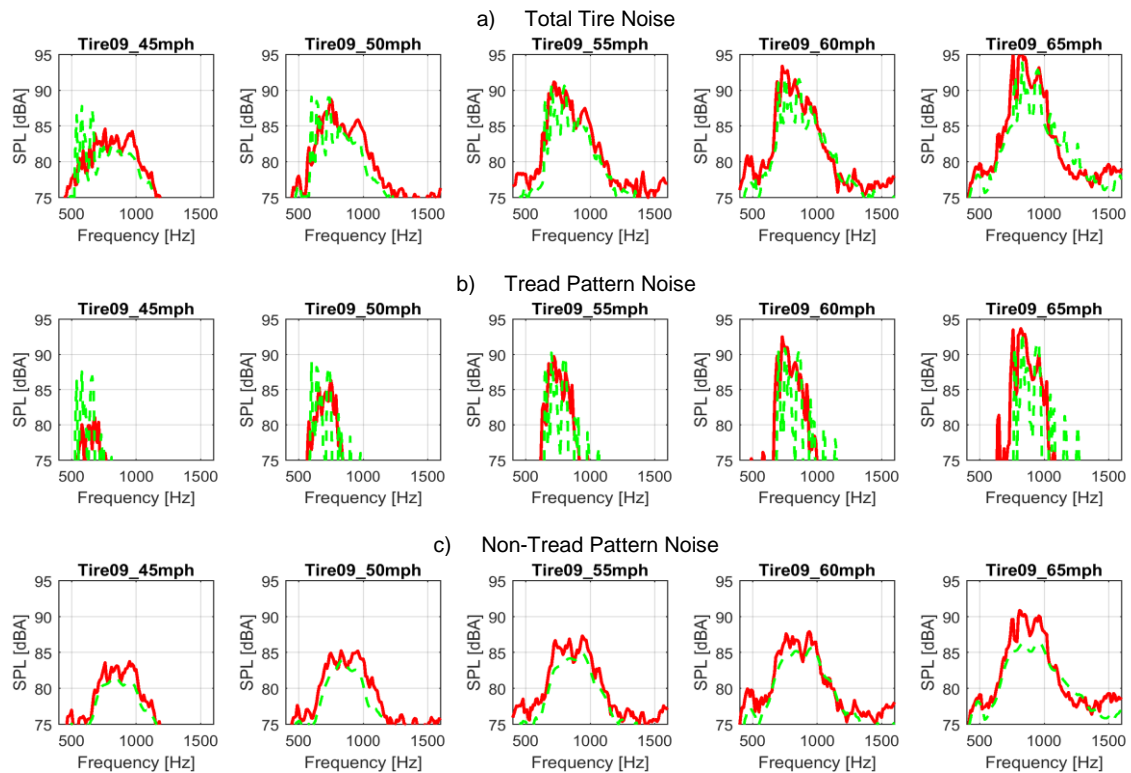


Figure 6 – Spectral validation for total, tread-pattern, and non-tread pattern noise of ANN TPIN noise modeling tool.

The predicted and measured overall A-weighted noise levels for all test tires at all speeds were also compared as shown in Figure 7. As observed, the overall total noise has an average error of 1.07 dB, while the tread-pattern noise has a 1.90 dB error, and finally the non-tread pattern noise error is of 1.02 dB. This proves a satisfactory accuracy for the developed tool.

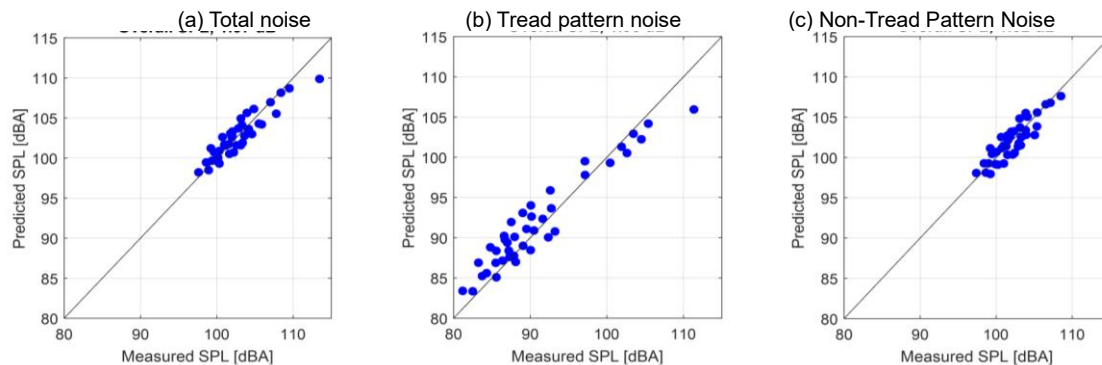


Figure 7 – Overall validation for total, tread-pattern, and non-tread pattern noise of ANN TPIN noise modeling tool.

FIA 2018

XI Congreso Iberoamericano de Acústica; X Congreso Ibérico de Acústica; 49º Congreso Español de Acústica -TECNIACUSTICA'18-
24 al 26 de octubre

Physical Based Prediction Model

A physically-based model to predict TPIN within the frequency range of interest is currently under development. The objective is to model the vibratory response of a rolling tire and couple it to the radiated noise. To this end, three main modeling stages are required. These are shown in Figure 8. First, the contact model takes into account the roughness of the pavement (or tire tread pattern) and the contact area to define the tire input excitation forces (or imposed displacements). The structural model then defines the dynamic behavior of the tire and the normal surface velocities of the tire for a given excitation input. Finally, the acoustic model computes the radiated noise from the normal surface velocities.

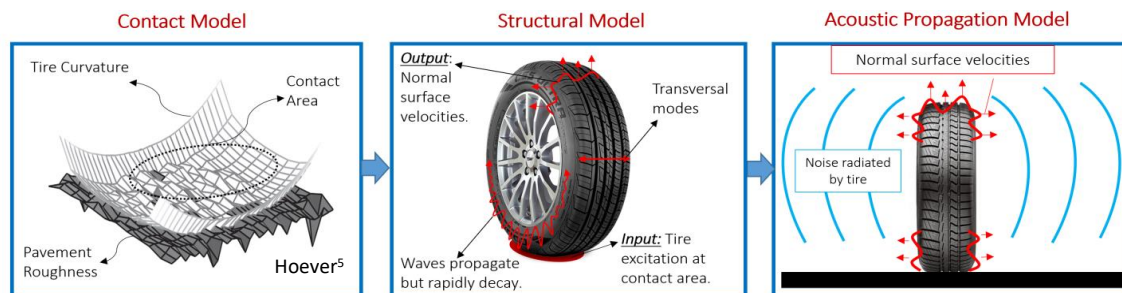


Figure 8 – Illustration of three main modeling stages.

Current research is mainly focused in the structural model of the tire. In this case, the tire curvature is ignored and it is unwrapped into a simply supported plate shown in Figure 9. The reason to do this is that TPIN dominant spectral content is expected to be above the ring frequency of the tire where curvature effects are not significant. The essential boundary conditions of the plate consist of simply supported edges due to the tire interaction with the rim. These define a modal behavior along the transversal direction of the tire. The tire is assumed infinite along circumferential direction in order to account for waves that are initially excited at the contact patch and propagate circumferentially along the tire, but rapidly decay due to damping and decaying characteristics of evanescent waves (see Figure 8). This is a reasonably good assumption since structural and noise measurements shown in the work by Donovan⁶ and Klos et al.⁷ suggest this behavior. The approach to solve the structural model is a modal analysis in the transverse direction and a wavenumber transform in the circumferential direction.

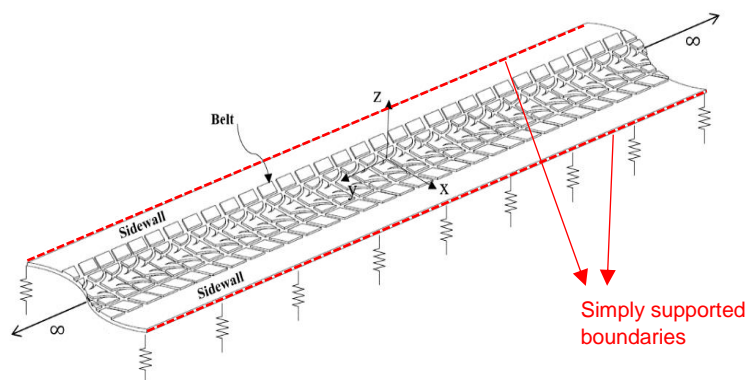


Figure 9 – Unwrapped representation of tire structure.

The equation of motion for this model is the following

$$-T_{0x} \frac{\partial^2 u}{\partial x^2} - T_{0y} \frac{\partial^2 u}{\partial y^2} + su + B_x \frac{\partial^4 u}{\partial x^4} + 2B_{xy} \frac{\partial^4 u}{\partial x^2 \partial y^2} + \frac{\partial^2}{\partial y^2} \left(B_y(y) \frac{\partial^2 u}{\partial y^2} \right) - m(y) \frac{\partial^2 u}{\partial t^2} = f(t) \delta(x - x_f) \delta(y - y_f) \quad (1)$$

FIA 2018

XI Congreso Iberoamericano de Acústica; X Congreso Ibérico de Acústica; 49º Congreso Español de Acústica -TECNIACUSTICA'18-
24 al 26 de octubre

where, T_{0x} and T_{0y} accounts for membrane tensions due to tire pressure; B_x , B_y , and B_{xy} correspond to circumferential, transversal and cross stiffness of the plate. On the other hand, s corresponds to the stiffness of the elastic bed, and m is the equivalent mass of the plate per unit area. The selected input to the system corresponds to a harmonic point force $f(t)$ located at the coordinates (x_f, y_f) .

Equation (1) shows that the transversal stiffness B_y and the mass per unit area of the tire m depend on y . In order to account for this, each transversal tire mode shape is defined as the summation of a set of continuous global admissible functions i.e. they cover the entire transversal domain of the tire. Figure 10 shows the typical behavior of these properties and how these affect the transversal mode shape for the frequencies of interest. It can be observed that the modal amplitude are reduced for the belt while the sidewalls vibration is larger. All used properties shown were obtained from the work by and Pinnington⁸ and Perisse et al.⁹. In addition, all results in this section are shown for a 155/70R13 tire.

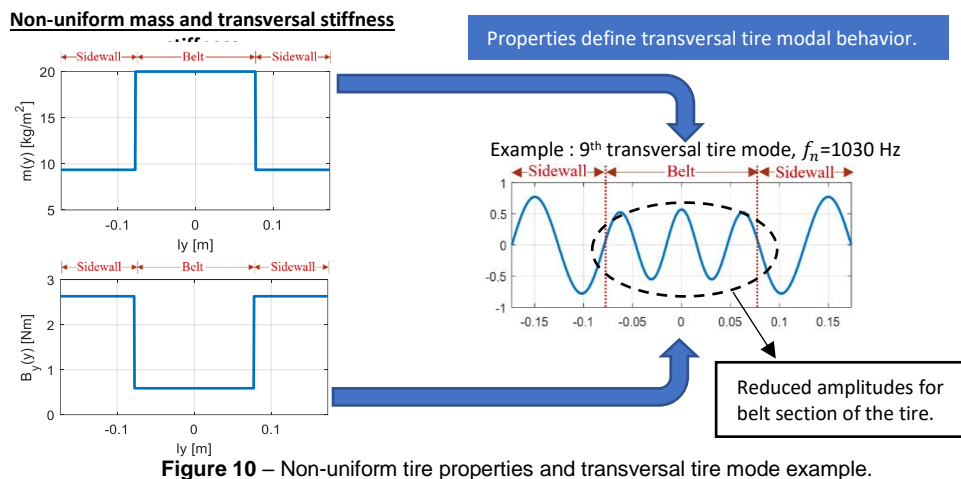


Figure 10 – Non-uniform tire properties and transversal tire mode example.

Figure 11a shows a time snapshot for the wave propagation approach to a harmonic (800 Hz) force ($F_0 = 4000$ N) at the tire center. In addition, a loss factor of 7% is implemented. The wave behavior of the tire response is very clear. For the sake of comparison, Figure 11b shows the tire response using a conventional modal solution with modes assumed along transversal and circumferential directions of the tire.

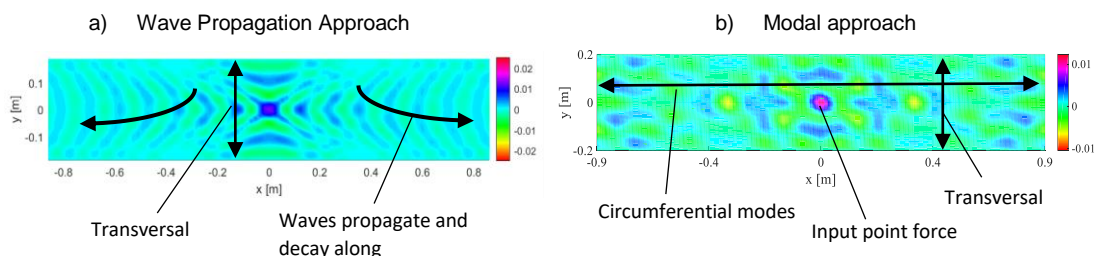


Figure 11 – Time Snapshot of: a) wave propagation and b) modal approach harmonic response.

The model is also capable of computing the frequency response of the normal surface velocity normalized by the input force anywhere on the tire surface. For example, Figure 12 shows these results along a line across the center transversal section of the tire. These results indicate a larger amplitude for the sidewall response over the frequency ranges of interest, as expected.

This physical model has the potential of capturing the tire dynamic response more accurately since its formulation is based on observed TPIN phenomena reported by many researchers. Thus, in the future, this noise prediction tool is expected to accurately predict structurally radiated noise.

FIA 2018

XI Congreso Iberoamericano de Acústica; X Congreso Ibérico de Acústica; 49º Congreso Español de Acústica -TECNIACUSTICA'18-
24 al 26 de octubre

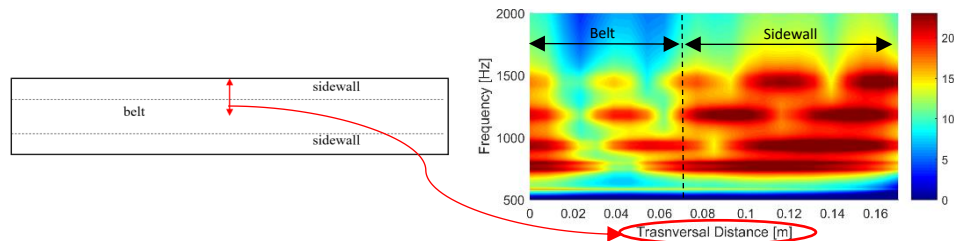


Figure 12 – Velocity frequency response function along transversal direction of the tire.

5. CONCLUSIONS

The experimental campaign conducted at Virginia Tech has uncovered new insight on TPIN behavior such as the existence of tread pattern and non-tread pattern related noise components not previously reported in the open literature. Finally, it has led to the development of a mathematical model that is able to accurately predict tire noise levels using ANNs. A physically-based model is also been developed with the potential of better capturing the tire's dynamic response and radiated noise.

6. ACKNOWLEDGMENTS

This work has been partially supported by the Center for Tire Research (CenTiRe), an NSF-I/UCRC (Industry/University Cooperative Research Centers) program led by Virginia Tech. The authors hereby wish to thank the industrial advisory board (IAB) of CenTiRe for their kind support and guidance. The authors also would like to thank Nexen Tire and Giti Tire for providing the test tires in this study, and to Hankook Tire for the digitization of the tire tread patterns. The OBSI system used in the experimental field tests was provided by AVEC, Inc., which is greatly appreciated. The pavement profile data was provided thanks to Vincent Bongioanni from VTTI. Finally, the authors would also like to acknowledge the collaborative efforts on code developments and field tests to Tan Li and Jianxiong Feng, former graduate students at Virginia Tech.

7. REFERENCES

- Bernhard R, Wayson RL, Haddock J, Neithalath N, El-Aassar A, Olek J, et al. An introduction to tire/pavement noise of asphalt pavement. Institute of Safe, Quiet and Durable Highways, Purdue University. 2005.
- Li T. Tire-Pavement Interaction Noise (TPIN) Modeling Using Artificial Neural Network (ANN) Blacksburg, VA: Virginia Polytechnic Institute and State University; 2017.
- Che Y, Xiao WX, Chen LJ, Huang ZC. GA-BP Neural Network Based Tire Noise Prediction. *Advanced Materials Research*. 2012;443-444:65-70.
- AASHTO, "Standard Method of Test for Measurement of Tire/Pavement Noise Using the On-Board Sound Intensity (OBSI) Method," AASHTO TP 76, 2013.
- C. Hoever. "The simulation of car and truck tyre vibrations, rolling resistance and rolling noise." (Doctor of Philosophy), Chalmers University of Technology Goteborg, Sweden (2014).
- P. R. Donavan and L. J. Oswald, "The Identification and Quantification of Truck Tire Noise Sources under On-Road Operating Conditions," in *General Motors Research Laboratories*, 1980, no. GMR-3380, pp. 253–8.
- J. Klos, F. Han, and R. Bernhard . "Response measurement of rolling tires using laser Doppler vibrometry". *Proceedings of Internoise*, Dearborn, MI, USA (2002).
- R. J Pinnington, "A wave model of a circular tyre. Part 1: belt modelling". *Journal of Sound and Vibration*, 290(1), 101-132, (2006).
- J. Perisse, J.M. Clairret and J.F. Hamet. "Modal testing of a smooth tire in low and medium frequency-estimation of structural parameters". *Proceedings of SPIE-The International Society for Optical Engineering*, San Antonio, Texas (2000).